IEEE Access
Multidisciplinary | Rapid Review | Open Access Journal

Received 16 July 2022, accepted 28 July 2022, date of publication 3 August 2022, date of current version 10 August 2022.

Digital Object Identifier 10.1109/ACCESS.2022.3195991

RESEARCH ARTICLE

Design of Robust Dynamic Output Feedback Event-Triggering Controllers for Nonlinear Uncertain Systems

SEONGCHEOL JEONG[1], JAEPIL BAN[2], (Member, IEEE), AND HARIM LEE[2]

[1]Department of Electrical Engineering, Pohang University of Science and Technology, Pohang, Gyeongbuk 37673, Republic of Korea
[2]School of Electronic Engineering, Kumoh National Institute of Technology, Gumi, Gyeongbuk 39177, Republic of Korea

Corresponding author: Jaepil Ban (jpban@kumoh.ac.kr)

This work was supported by the National Research Foundation of Korea (NRF) grant funded by the Korea Government [Ministry of Science and ICT (MSIT)] under Grant NRF-2022R1G1A1007058.

ABSTRACT This paper presents a design of dynamic output feedback event-triggering control for nonlinear uncertain networked control systems. The plant and actuator asynchronously transmit the measurement and control signals over two different communication channels. We address the norm-bounded time-varying parameter uncertainties in a nonlinear plant. First, considering the exogenous disturbances and noises in the control and measurement signals, sufficient conditions for the $\mathcal{L}_2$ stability of the nonlinear networked control systems are given in the presence of the uncertainties. Then, we propose design conditions to choose the dynamic output feedback control and triggering laws in terms of linear matrix inequalities (LMIs). The proposed conditions enable the controller and event-triggering parameters to be jointly optimized to lessen the number of transmissions, guaranteeing a certain level of $\mathcal{L}_2$ gain. Numerical examples demonstrate the effectiveness of the proposed method.

INDEX TERMS Hybrid dynamical systems, $\mathcal{L}_2$-stability, linear matrix inequality, networked control systems, nonlinear uncertain systems.

I. INTRODUCTION

Networked control systems (NCSs) are widely applied in many fields due to their attractive advantages, such as reduced system wiring, low weight and space, ease of system diagnosis and maintenance, and increased system agility, see [1]–[8]. In NCSs, reducing the amount of transmission data is essential because data congestion at routers can cause severe time delay or packet losses, e.g., [9]. In traditional NCSs, sampled-data control systems, the control input and measurement output signals are sampled and transmitted periodically even when the sampled values do not change, expanding communication resource and power usage.

Event-triggered control (ETC) has been proposed to overcome this issue, as in [10], [11]. The ETC systems prevent excessive use of the communication by adapting transmissions to the current signal so that the network is only used when it is necessary, see [12]–[14]. An adaptive event-triggered fault-tolerant tracking control problem was investigated for a class of MIMO uncertain nonlinear systems with unknown nonlinearities and actuator faults in [15]. [16] addressed an event-triggered adaptive control method to reduce the communication and computational resources of uncertain nonlinear systems with unknown control directions and actuator faults, while eliminating the explosion of complexity problem in backstepping. [17] was devoted to the event-triggered adaptive control design without any priori knowledge of the signs of unknown virtual control coefficients for uncertain nonlinear systems with full state constraints. In [18], $\mathcal{H}_\infty$ static output feedback tracking control methodology was proposed for discrete-time nonlinear networked systems subject to quantization effects and asynchronous event-triggered constraints.

One challenge in designing an ETC is combining the triggering condition with the feedback control law. Many existing event-triggering strategies have been developed using the

The associate editor coordinating the review of this manuscript and approving it for publication was Zhiguang Feng.

emulation approach, see [14], [19], [20]. In this approach, the feedback law is first synthesized to stabilize the plant without any network communication. Subsequently, a sampling rule is constructed, reducing network communication. The approach is intuitive and easy to understand but can limit the control performance, e.g., $\mathcal{L}_2$-gain, due to an initial choice on the feedback law. [21]–[23] and [24] have proposed co-design methods that choose both the control law and triggering conditions simultaneously. Many studies on event-triggering controller designs have investigated full-state feedback controllers. However, in many real-world control applications, only partial state is measurable. Thus, it is important to study output-based ETC, see [25].

Recently, researchers have studied the co-designing of feedback control and event-triggering laws. Based on the analysis in [26], [27] proposed an co-design method of dynamic output feedback (DOF) and event-triggering laws using linear matrix inequalities (LMIs). Furthermore, they formulated an optimization problem using the proposed LMIs to decrease the number of transmissions. [28] proposed a less conservative co-design method of the output feedback law and event-triggering conditions by presenting three additional constraints. It is worth noting that the aforementioned works considered ideal linear systems. However, many practical systems are described as nonlinear systems. In addition, parameter uncertainties in the system model can deteriorate the static and dynamic performances if not considered in the controller design, see [29]–[32]. Furthermore, [33], [34] reported that even when the magnitude of disturbances is tiny, there may be no positive minimum inter-event times for event-triggering mechanisms.

Motivated by the above discussions, this paper presents an effective co-design strategy for a robust DOF law and triggering conditions for nonlinear uncertain systems. The ETC systems consist of a nonlinear uncertain plant, controller, and communication network. The plant output and control input are transmitted to the controller and the actuators asynchronously. Considering a nonlinear ETC systems with norm-bounded time-varying parameter uncertainties, we provide the LMI-based $\mathcal{L}_2$ stability analysis. Moreover, we propose LMI-based sufficient conditions for the co-design of DOF law and triggering conditions. Subsequently, a convex optimization problem is presented for a class of nonlinear uncertain ETC systems to reduce the number of transmissions, guaranteeing a certain level of $\mathcal{L}_2$ gain. In contrast to the previously published work [26], we can optimize the DOF controller and triggering laws using the proposed LMI conditions. We present numerical examples to show the effectiveness of the proposed design methodology. The main contributions of this study are summarized as follows:

1) This study firstly addresses the co-design methodology of the DOF control and event-triggering laws for nonlinear uncertain systems.
2) We deal with more real-world situations by investigating research on the ETC systems that are asynchronously triggered on controller and actuator over two different communication channels.
3) We provide sufficient conditions for the $\mathcal{L}_2$ stability of the nonlinear ETC systems in the presence of the time-varying norm-bounded uncertainties.
4) A convex optimization problem using the proposed LMI conditions is presented to lessen the number of transmissions.

The rest of this paper is organized as follows. Section II presents the preliminaries for modeling the event-triggered nonlinear uncertain plant. Section III provides the LMI-based $\mathcal{L}_2$ stability analysis. Subsequently, we present the design methodology of event-triggering DOF controllers and an optimization method to minimize the amount of transmission data. The numerical simulations are presented in Section IV. Finally, the conclusions are made in Section V.

II. PROBLEM STATEMENT

A. PRELIMINARIES

Let $\mathbb{R} := (-\infty, \infty)$, $\mathbb{R}_{\geq 0} := [0, \infty)$, $\mathbb{Z}_{\geq 0} := \{0, 1, 2, ..\}$ and $\mathbb{Z}_{>0} := \{1, 2, ..\}$. We denote the transpose and inverse of the transpose of A as A^T and A^{-T}, respectively. We represent block-diagonal matrix with the entries $A_1, \cdots, A_N$ on the diagonal as $\mathrm{diag}(A_1, \cdots, A_N)$. The symbol $\star$ denotes the symmetric blocks. The minimum and maximum eigenvalues of the symmetric matrix A are denoted as $\lambda_{min}(A)$ and $\lambda_{max}(A)$, respectively. A continuous function $\gamma : \mathbb{R}_{\geq 0}$ is of class $\mathcal{K}$ if it is zero at zero, strictly increasing, and it is of class $\mathcal{K}_\infty$ if $\gamma(s) \to \infty$ as $s \to \infty$. We use (x, y) to represent the vector $[x^T, y^T]^T$ for $x \in \mathbb{R}^n$ and $y \in \mathbb{R}^m$. For a vector $x \in \mathbb{R}^n$, we denote $\|x\| = \sqrt{x^T x}$ as its Euclidean norm.

In this study, the hybrid dynamical system framework was used to reprsent event-triggering control systems:

$$\begin{aligned} \dot{x} &= F(x, w) \quad x \in \mathcal{F}, \\ x^+ &\in G(x, w) \quad x \in \mathcal{J}, \end{aligned} \tag{1}$$

where $x \in \mathbb{R}^{n_x}$ is the state vector, $w \in \mathbb{R}^{n_w}$ is the external disturbance, F and G represent the flow and jump maps, respectively. For x in the flow set $\mathcal{F}$, x obeys the continuous dynamics $F(x, w)$; for x in the jump set $\mathcal{J}$, x obeys the discrete dynamics $G(x, w)$. For the details on hybrid dynamical systems, please see [35], [36]. We use the following definitions of $\mathcal{L}_2$ norm of hybrid signals and $\mathcal{L}_2$ stability for systems in the rest of the paper, see [27].

Definition 1: For a hybrid signal z defined on the hybrid time domain $\mathrm{dom}\, z = \cup_{j=0}^{J-1} \left[t_j, t_{j+1}\right] \times \{j\}$ with J possibly ∞ or $t_J = \infty$, the $\mathcal{L}_2$ norm of z is defined as $\|z\|_2 = \left(\sum_{j=0}^{J-1} \int_{t_j}^{t_{j+1}} |z(t, j)|^2 dt\right)^{\frac{1}{2}}$, provided that the right-hand side exists and is finite, where $z \in \mathcal{L}_2$.

Definition 2: System (1) is $\mathcal{L}_2$ stable from the input (w) to the output $z = h(x, w)$ with gain less than or equal to $\gamma \geq 0$ if there exists $\beta \in \mathcal{K}_\infty$ such that any solution pair (x, w) to (1) satisfies $\|z\|_2 \leq \beta\left(|x(0, 0)|\right) + \gamma \|w\|$.

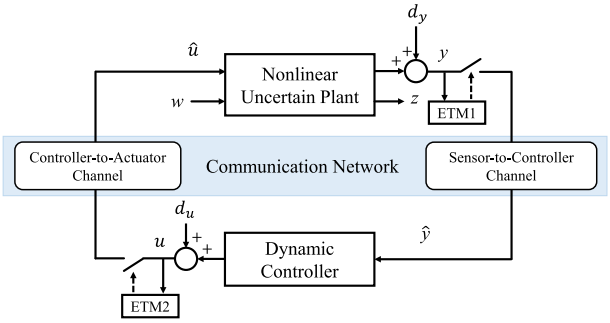

FIGURE 1. Schematic diagram of the event-triggered control system.

B. REPRESENTATION OF EVENT-TRIGGERED CONTROL SYSTEMS

We consider an ETC system where the controller and plant send signals through digital channels in a shared communication network (Fig. 1). We represent the nonlinear uncertain plant as follows:

$$\dot{x}_p = A_p x_p + B_f f(x_p) + B_p \hat{u} + E_p w \tag{2a}$$
$$y = C_p x_p + d_y, \tag{2b}$$

where $x_p \in \mathbb{R}^{n_p}$ is the plant state, $\hat{u} \in \mathbb{R}^{n_u}$ is the sampled value of the control input $u \in \mathbb{R}^{n_u}$, $w \in \mathcal{L}_2[0,\infty)$ is the external disturbance, $y \in \mathbb{R}^{n_y}$ is the measured output, and $d_y \in \mathbb{R}^{n_y}$ is the measurement noise. We consider a plant that includes model uncertainty. A_p is represented by the sum of the nominal plant matrix A_{p0} and the time-varying parametric uncertainty $\Delta A_p(t)$ that is represented as $E_{p\Delta}\Delta_p(t)F_{p\Delta}$, i.e., $A_p = A_{p0} + E_{p\Delta}\Delta_p F_{p\Delta}$ with $\Delta_p^T\Delta_p \le I$. $f(x_p) \in \mathbb{R}^{n_f}$ is a nonlinear function that satisfies β-Lipschitz with respect to x, i.e., $\forall x, y \in \mathbb{R}^n$, $\|f(x) - f(y)\| \le \beta\|x - y\|$ where $\beta > 0$ is the Lipschitz constant.

The DOF controller which is described in Fig. 1 is given as follows:

$$\dot{x}_c = A_c x_c + B_c \hat{y} \tag{3a}$$
$$u = C_c x_c + d_u, \tag{3b}$$

where $x_c \in \mathbb{R}^{n_c}$ is the controller state, $\hat{y} \in \mathbb{R}^{n_y}$ is the last transmitted value of the output measurement $y \in \mathbb{R}^{n_y}$, and $d_u \in \mathbb{R}^{n_u}$ is the noise corrupting the control input. The noise d_u may include model computational glitches, quantization errors, or, more generally, any disturbance which may affect the control input. We assume that the noise signals $d_y \in \mathbb{R}^{n_y}$ and $d_u \in \mathbb{R}^{n_u}$ that affect y and u, respectively, are absolutely continuous; their time-derivatives exist for almost all points in time and are in $\mathcal{L}_2$.

In Fig 1, event-triggering mechanisms 1 (ETM1) and 2 (ETM2) govern the control input and measurement output data transmissions, respectively. For example, ETM1 allows sending measurement output y over the network only when $t = t_i^y$, $i \in \mathbb{Z}_{\ge 0}$. Subsequently, the most recently transmitted data is kept constant at the receiver's side employing a zero-order hold element (Fig. 2). ETM2 operates similar

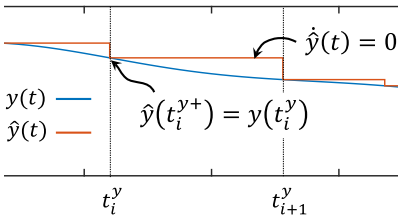

FIGURE 2. Input data transmission of the event-triggered control system.

to ETM1 in the control input data transmission but works asynchronously with ETM1. The ETM2 allows sending u through the network at $t = t_i^u$, $i \in \mathbb{Z}_{\ge 0}$, otherwise, the transmission is prevented. Thus, we can model the signal transmissions through the communication network can be modeled as following:

$$\dot{\hat{y}} = 0 \quad t \in [t_i^y, t_{i+1}^y] \tag{4a}$$
$$\dot{\hat{u}} = 0 \quad t \in [t_i^u, t_{i+1}^u] \tag{4b}$$
$$\dot{\tau}_y = 1 \quad t \in [t_i^y, t_{i+1}^y] \tag{4c}$$
$$\dot{\tau}_u = 1 \quad t \in [t_i^u, t_{i+1}^u] \tag{4d}$$
$$\hat{y}(t_i^{y+}) = y(t_i^y), \quad \tau_y(t_i^{y+}) = 0, \tag{4e}$$
$$\hat{u}(t_i^{u+}) = u(t_i^u), \quad \tau_u(t_i^{u+}) = 0, \tag{4f}$$

where τ_y and τ_u are the elapsed times since the most recent transmission instant of the measured output and control input, respectively. The transmission instants are determined by triggering laws whose design method is presented below.

Remark 1: Several existing studies have dealt with situations in which the communication networks are synchronized, see [37]–[39]. However, in practical applications, there are limitations such as physical distance and hardware differences between the two channels. Taking this into account, we investigate more practical situations by addressing the ETC system in which two different communication channels are asynchronously triggered on controller and actuator, as described in (4).

Let us define the network-induced errors as $e_y = \hat{y} - y$, $e_u = \hat{u} - u$, and $e = (e_y, e_u)$. Let $\bar{x} := (x, e_y, e_u, \tau_y, \tau_u) \in \mathbb{R}^{n_{\bar{x}}}$ with $x := (x_p, x_c) \in \mathbb{R}^{n_x}$, $\bar{w} := (w, d_y, d_u) \in \mathbb{R}^{n_{\bar{w}}}$, $\bar{d} := (\dot{d}_y, \dot{d}_u) \in \mathbb{R}^{n_{\bar{d}}}$, and $\xi := (\bar{w}, \bar{d})$. Then, by using the hybrid system framework, the whole ETC system dynamics (2)–(4) is presented as follows:

$$\dot{\bar{x}} = \begin{pmatrix} \bar{f}_1(x, e, \xi) \\ \bar{f}_2(x, e, \xi) \\ \bar{f}_3(x, e, \xi) \\ 1 \\ 1 \end{pmatrix} \qquad \bar{x} \in \mathcal{F}_y \cap \mathcal{F}_u \tag{5a}$$

$$\bar{x}^+ \in \begin{cases} [I]\{(x, 0, e_u, 0, \tau_u)\} & [I]\bar{x} \in \mathcal{J}_y \backslash \mathcal{J}_u \\ \{(x, e_y, 0, \tau_y, 0)\} & \bar{x} \in \mathcal{J}_u \backslash \mathcal{J}_y \\ \{(x, 0, 0, 0, 0)\} & \bar{x} \in \mathcal{J}_y \cap \mathcal{J}_u, \end{cases} \tag{5b}$$

where

$$\begin{aligned}
\bar{f}_1(x,e,\xi) &= A_1x + R_1f(x_p) + B_1e_y + M_1e_u + E_1\bar{w},\\
\bar{f}_2(x,e,\xi) &= A_2x + R_2f(x_p) + M_2e_u + E_2\bar{w} + F_2\bar{d},\\
\bar{f}_3(x,e,\xi) &= A_3x + B_3e_y + E_3\bar{w} + F_3\bar{d},\\
A_1 &= A_{10} + \Delta A_1, \quad A_{10} = \begin{bmatrix} A_{p0} & B_pC_c \\ B_cC_p & A_c \end{bmatrix},\\
\Delta A_1 &= \begin{bmatrix} \Delta A_p & 0 \\ 0 & 0 \end{bmatrix} = E_\Delta \Delta_p F_\Delta, \quad E_\Delta = \begin{bmatrix} E_{p\Delta} \\ 0 \end{bmatrix},\\
F_\Delta &= \begin{bmatrix} F_{p\Delta} & 0 \end{bmatrix}, \quad R_1 = \begin{bmatrix} B_f^T & 0 \end{bmatrix}^T = B_f U_p^T,\\
B_1 &= \begin{bmatrix} 0 \\ B_c \end{bmatrix}, \quad M_1 = \begin{bmatrix} B_p \\ 0 \end{bmatrix}, \quad E_1 = \begin{bmatrix} E_p & 0 & B_p \\ 0 & B_c & 0 \end{bmatrix},\\
A_2 &= -C_yA_1, \quad R_2 = -C_yR_1, \quad M_2 = -C_yM_1,\\
E_2 &= -C_yE_1, \quad F_2 = \begin{bmatrix} -I & 0 \end{bmatrix}, \quad A_3 = -C_uA_1,\\
B_3 &= -C_uB_1, \quad E_3 = -C_uE_1, \; F_3 = \begin{bmatrix} 0 & -I \end{bmatrix},\\
C_y &= \begin{bmatrix} C_p & 0 \end{bmatrix}, \quad C_u = \begin{bmatrix} 0 & C_c \end{bmatrix}, \; U_p = \begin{bmatrix} I & 0 \end{bmatrix}.
\end{aligned}$$

The standard form of the ETC flow and jump sets is as follows:

$$\begin{aligned}
\mathcal{F}_y &= \left\{\bar{x} : |e_y| \le \eta_y|y| \text{ or } \tau_y \in \left[0, T_y\right]\right\}\\
\mathcal{J}_y &= \left\{\bar{x} : |e_y| \ge \eta_y|y| \text{ and } \tau_y \ge T_y\right\}\\
\mathcal{F}_u &= \{\bar{x} : |e_u| \le \eta_u|u| \text{ or } \tau_u \in [0, T_u]\}\\
\mathcal{J}_u &= \{\bar{x} : |e_u| \ge \eta_u|u| \text{ and } \tau_u \ge T_u\},
\end{aligned} \tag{6}$$

where $\eta_u,\ \eta_y \ge 0$ are the parameters to be designed. $T_y \in (0, \bar{T}_y(\zeta_y))$ and $T_u \in (0, \bar{T}_u(\zeta_u))$ denotes the minimum inter-event times between two consecutive transmissions of y and u, respectively, where $\bar{T}_y(\zeta_y) = \frac{1}{\zeta_y}\frac{\pi}{2}$ and $\bar{T}_u(\zeta_u) = \frac{1}{\zeta_u}\frac{\pi}{2}$, preventing Zeno behavior. ζ_y and ζ_u are design parameters, see [27]. The error dynamics $\dot{e}_y = f_3(e, x, \xi)$ also includes uncertainties from the plant, making the controller design difficult. We define the controlled output as

$$z = [C_z^p \;\; 0]x + [D_z^w \;\; D_z^y \;\; D_z^u]\bar{w} = C_zx + D_z\bar{w}, \tag{7}$$

where $C_z^p, D_z^w, D_z^y, D_z^u$ are matrices with appropriate dimensions.

III. MAIN RESULTS

A. STABILITY ANALYSIS

In this subsection, we present sufficient conditions for the $\mathcal{L}_2$ stability of the system (5). Before we present our main theorem, we present the following lemma that is used for the proof of the main theorem.

Lemma 1: Consider system (5) with the flow and jump sets defined in (6) and the output z in (7). For given $T_y \in (0, \bar{T}_y(\zeta_y))$ and $T_u \in (0, \bar{T}_u(\zeta_u))$, suppose that there exist the locally Lipschitz functions $V : \mathbb{R}^{n_x} \to \mathbb{R}_{\ge 0}$, $W_y : \mathbb{R}^{n_y} \to \mathbb{R}_{\ge 0}$, $W_u : \mathbb{R}^{n_u} \to \mathbb{R}_{\ge 0}$ with W_y, W_u positive definite, continuous functions $H_y : \mathbb{R}^{n_x+n_{e_u}+n_\xi} \to \mathbb{R}_{\ge 0}$, $H_u : \mathbb{R}^{n_x+n_{e_y}+n_\xi} \to \mathbb{R}_{\ge 0}$, real numbers $\eta_{\bar{w}}^2, \eta_{\bar{d}}^2 \in \mathbb{R}$, L_y, $L_u \ge 0$, $\gamma_y, \gamma_u > 0$, $\underline{\alpha}, \overline{\alpha} \in \mathcal{K}_\infty$, a continuous function $\delta_y : \mathbb{R}^{n_y} \to \mathbb{R}_{\le 0}$, $\delta_u : \mathbb{R}^{n_u} \to \mathbb{R}_{\le 0}$, $\alpha_s : \mathbb{R}^{n_x+n_\xi} \to \mathbb{R}$ such that

(i) for all $x \in \mathbb{R}^{n_x}$

$$\underline{\alpha}(|x|) \le V(x) \le \overline{\alpha}(|x|) \tag{8}$$

(ii) for almost all $x \in \mathbb{R}^{n_x}$ and all $(e, \xi) \in \mathbb{R}^{n_e+n_\xi}$

$$\begin{aligned}
\langle \nabla V(x), \bar{f}_1(x,e,\xi)\rangle \le\ & -\alpha_s(x,\xi) - H_y^2(x,e_u,\xi)\\
& - H_u^2(x,e_y,\xi) - \delta_y(y) - \delta_u(u)\\
& + \gamma_y^2W_y^2(e_y) + \gamma_u^2W_u^2(e_u)
\end{aligned} \tag{9}$$

(iii) for almost all $e \in \mathbb{R}^{n_e}$ and all $(x, \xi) \in \mathbb{R}^{n_x+n_\xi}$

$$\begin{aligned}
\langle \nabla W_y(e_y), \bar{f}_2(x,e,\xi)\rangle &\le L_yW_y(e_y) + H_y(x,e_u,\xi)\\
\langle \nabla W_u(e_u), \bar{f}_3(x,e,\xi)\rangle &\le L_uW_u(e_u) + H_u(x,e_y,\xi)
\end{aligned} \tag{10}$$

where $\alpha_s(x, \bar{w}, \bar{d}) := |z|^2 - \eta_{\bar{w}}^2|\bar{w}|^2 - \eta_{\bar{d}}^2|\bar{d}|^2$. Then, system (5) is $\mathcal{L}_2$-stable from ξ to z with an $\mathcal{L}_2$ gain less than or equal to $\eta = \sqrt{\max\left\{\eta_{\bar{w}}^2, \eta_{\bar{d}}^2\right\}}$.

Proof: The proof uses a similar procedure to that in [26]. Thus, this is omitted here.

Remark 2: Lemma 1 disassociates ξ into $\bar{w}$ and $\bar{d}$ compared with Assumption 2 in [26]. Moreover, we introduce the functions H_y and H_u which also depend on the errors e_u and e_y, respectively, enabling (9) and (10) to be less conservative.

Now, we propose the following theorem that addresses the $\mathcal{L}_2$-gain analysis of the ETC systems (5) with the flow and jump sets defined in (6).

Theorem 1: Consider system (5) with the flow and jump sets defined in (6) and the output z in (7). Suppose that there exist scalars $\varepsilon_y,\ \varepsilon_u,\ \beta,\ \mu_y,\ \mu_u,\ \gamma_{\bar{w}},\ \gamma_{\bar{d}},\ \lambda_y,\ \lambda_u > 0$, $\rho \ge 0$ and a positive definite matrix P such that

$$\Psi < 0, \tag{11}$$

where $\Psi = \left\{\Psi_{ij}\right\}$, $i, j \in \{1, 2, \ldots, 6\}$ is the symmetric matrix whose components are given as following matrices:

$$\begin{aligned}
\Psi_{11} &= A_1^TP + PA_1 + C_z^TC_z + \lambda_y^2A_2^TA_2 + \lambda_u^2A_3^TA_3\\
&\quad + \varepsilon_yC_y^TC_y + \varepsilon_uC_u^TC_u + \rho\beta U_p^TU_p,\\
\Psi_{21} &= R_1^TP + \lambda_y^2R_2^TA_2, \quad \Psi_{22} = -\rho I + \lambda_y^2R_2^TR_2\\
\Psi_{31} &= B_1^TP + \lambda_u^2B_3^TA_3, \quad \Psi_{33} = -\mu_yI + \lambda_u^2B_3^TB_3,\\
\Psi_{41} &= M_1^TP + \lambda_y^2M_2^TA_2, \quad \Psi_{42} = \lambda_y^2M_2^TR_2,\\
\Psi_{44} &= -\mu_uI + \lambda_y^2M_2^TM_2,\\
\Psi_{51} &= E_1^TP + D_z^TC_z + \lambda_y^2E_2^TA_2 + \lambda_u^2E_3^TA_3\\
&\quad + \varepsilon_yD_y^TC_y + \varepsilon_uD_u^TC_u,\\
\Psi_{52} &= \lambda_y^2E_2^TR_2, \quad \Psi_{53} = \lambda_u^2E_3^TB_3,\\
\Psi_{54} &= \lambda_y^2E_2^TM_2,\\
\Psi_{55} &= -\gamma_{\bar{w}}I + D_z^TD_z + \lambda_y^2E_2^TE_2 + \lambda_u^2E_3^TE_3 + \varepsilon_yD_y^TD_y\\
&\quad + \varepsilon_uD_u^TD_u,\\
\Psi_{61} &= \lambda_y^2F_2^TA_2 + \lambda_u^2F_3^TA_3, \; \Psi_{62} = \lambda_y^2F_2^TR_2\\
\Psi_{63} &= \lambda_u^2F_3^TB_3, \quad \Psi_{64} = \lambda_y^2F_2^TM_2
\end{aligned}$$

$$\Psi_{65} = \lambda_y^2 F_2^T E_2 + \lambda_u^2 F_3^T E_3,$$
$$\Psi_{66} = -\gamma_{\bar{d}} I + \lambda_y^2 F_2^T F_2 + \lambda_u^2 F_3^T F_3,$$
$$D_u = [0 \quad 0 \quad I], \quad D_y = [0 \quad I \quad 0].$$

Let the parameters in (6) and $\bar{T}_y(\zeta_y)$,$\bar{T}_u(\zeta_u)$ be chosen as $\eta_y = \sqrt{\frac{\varepsilon_y}{\mu_y}}$, $\eta_u = \sqrt{\frac{\varepsilon_u}{\mu_u}}$, $\zeta_y = \frac{\sqrt{\mu_y}}{\lambda_y}$, and $\zeta_u = \frac{\sqrt{\mu_u}}{\lambda_u}$. Then, system (5) with (6) is $\mathcal{L}_2$-stable from $(\bar{w}, \bar{d})$ to z with an $\mathcal{L}_2$-gain less than or equal to $\gamma = \sqrt{\max\{\gamma_{\bar{w}}, \gamma_{\bar{d}}\}}$.

Proof: Please see the Appendix.

Remark 3: In this paper, we derive the results of the $\mathcal{L}_2$ stability analysis of the nonlinear system (5) while that of [26] (Proposition 1) was addressed for a linear system. In addition, we provide less conservative condition (11) with the separated disturbances $\bar{w}$, $\bar{d}$ and the functions H_y and H_u which have the error terms e_u and e_y, respectively.

We use condition (11) to derive sufficient conditions for designing ETC. However, we face two challenges while achieving this: 1) the nonlinear terms $A_2^T A_2$ and $A_3^T A_3$ make the LMI relaxation of (11) difficult using standard LMI relaxation methods when we set the control law, A_c, B_c, and C_c, as decision variables (see, [27], [28]). [27], [28] put some additional LMI constraints to obtain LMI conditions. However, the obtained LMI conditions are only available on ideal linear systems; 2) in condition (11), A_1 includes the uncertainty ΔA_1, i.e.; $A_1 = A_{10} + \Delta A_1$. Thus, A_2 and A_3 also include ΔA_1, making the LMI relaxation difficult. In the next subsection, we provide a robust ETC design for nonlinear systems with parameter uncertainties in the system model.

B. CONTROLLER DESIGN

In this subsection, a new controller design scheme for the output feedback and triggering laws is proposed for robust ETC of nonlinear uncertain plants. We present the following theorem that provides the LMI-based design conditions and procedures to obtain the controller parameters.

Theorem 2: Consider system (5) with (6) and its controlled output (7). For positive scalars α_1, α_2, α_3, $\gamma_{\bar{d}}$, λ_y, and λ_u, the $\mathcal{L}_2$-gain $(\bar{w}, \bar{d})$ to z of the system (5) with (6) is less than or equal to $\gamma = \sqrt{\max\{\gamma_{\bar{w}}, \gamma_{\bar{d}}\}}$, if there exist scalars β, ν, μ_y, μ_u, σ_y, σ_u, $\gamma_{\bar{w}} > 0$, and $\rho \geq 0$, matrices $\hat{A}_c$, $\hat{B}_c$, $\hat{C}_c$, and positive definite matrices X, Y, H_1, H_2, H_3 with appropriate dimensions such that

$$\Omega < 0, \quad (12)$$
$$\begin{bmatrix} I & \star & \star \\ 0 & I & \star \\ \lambda_y^2 \Phi_6^T & \lambda_u^2 \Phi_7^T & 2\alpha_1 \Phi_{12} - H_1 \end{bmatrix} \geq 0, \quad (13)$$
$$\begin{bmatrix} I & \star \\ \Phi_6^T & 2\alpha_2 \Phi_{12} - H_2 \end{bmatrix} \geq 0, \quad (14)$$
$$\begin{bmatrix} I & \star \\ \Phi_7^T & 2\alpha_3 \Phi_{12} - H_3 \end{bmatrix} \geq 0, \quad (15)$$

where $\Omega = \{\Omega_{i,j}\}$, $i, j \in \{1, 2, \ldots, 14\}$ is the symmetric matrix whose components are given as follows:

$$\begin{aligned}
\Omega_{1,1} &= \Phi_1 + \Phi_1^T, \quad \Omega_{2,1} = \Phi_2, \quad \Omega_{2,2} = -\rho I, \\
\Omega_{3,1} &= \Phi_3, \quad \Omega_{3,3} = -\mu_y I, \quad \Omega_{4,1} = \Phi_4, \\
\Omega_{4,4} &= -\mu_u I, \\
\Omega_{5,1} &= \Phi_5, \quad \Omega_{5,5} = -\gamma_{\bar{w}} I, \\
\Omega_{6,1} &= \Omega_{7,1} = \Omega_{8,1} = \Phi_1, \\
\Omega_{6,2} &= \Omega_{7,2} = \Phi_2^T, \quad \Omega_{6,3} = \Omega_{8,3} = \Phi_3^T, \\
\Omega_{6,4} &= \Omega_{7,4} = \Phi_4^T, \quad \Omega_{6,5} = \Omega_{7,5} = \Omega_{8,5} = \Phi_5^T, \\
\Omega_{6,6} &= -\frac{\tilde{\gamma}_{\bar{d}}}{\alpha_1^2} H_1, \quad \Omega_{7,7} = -(\alpha_2 \lambda_y)^{-2} H_2, \\
\Omega_{8,8} &= -(\alpha_3 \lambda_u)^{-2} H_3, \\
\Omega_{9,1} &= \Phi_6, \quad \Omega_{9,5} = D_y, \quad \Omega_{9,9} = -\sigma_y I, \\
\Omega_{10,1} &= \Phi_7, \quad \Omega_{10,5} = D_u, \quad \Omega_{10,10} = -\sigma_u I, \\
\Omega_{11,1} &= \Phi_8, \quad \Omega_{11,5} = D_z, \quad \Omega_{11,11} = -I, \\
\Omega_{12,1} &= \Phi_9, \quad \Omega_{12,12} = -(\rho\beta)^{-1} I, \\
\Omega_{13,1} &= \Omega_{13,6} = \Omega_{13,7} = \Omega_{13,8} = \Phi_{10}, \\
\Omega_{13,13} &= -\nu^{-1} I, \\
\Omega_{14,1} &= \Phi_{11}, \quad \Omega_{14,14} = -\nu I, \\
\Phi_1 &= \begin{bmatrix} YA_{p0} + \hat{B}_c C_p & \hat{A}_c \\ A_{p0} & A_{p0} X + B_p \hat{C}_c \end{bmatrix}, \\
\Phi_2 &= \begin{bmatrix} B_f^T Y & B_f^T \end{bmatrix}, \quad \Phi_3 = \begin{bmatrix} \hat{B}_c^T & 0 \end{bmatrix}, \\
\Phi_4 &= \begin{bmatrix} B_p^T Y & B_p^T \end{bmatrix}, \quad \Phi_5 = \begin{bmatrix} E_p^T Y & E_p^T \\ \hat{B}_c^T & 0 \\ B_p^T Y & B_p^T \end{bmatrix}, \\
\Phi_6 &= \begin{bmatrix} C_p & C_p X \end{bmatrix}, \quad \Phi_7 = \begin{bmatrix} 0 & \hat{C}_c \end{bmatrix}, \\
\Phi_8 &= \begin{bmatrix} C_z^p & C_z^p X \end{bmatrix}, \quad \Phi_9 = \begin{bmatrix} I & X \end{bmatrix}, \\
\Phi_{10} &= \begin{bmatrix} E_{p\Delta}^T Y & E_{p\Delta}^T \end{bmatrix}, \quad \Phi_{11} = \begin{bmatrix} F_{p\Delta} & F_{p\Delta} X \end{bmatrix}, \\
\Phi_{12} &= \begin{bmatrix} Y & I \\ I & X \end{bmatrix}, \quad \tilde{\gamma}_{\bar{d}} = \gamma_{\bar{d}} - \max\{\lambda_y^2, \lambda_u^2\}.
\end{aligned}$$

Moreover, the control law A_c, B_c, and C_c can be calculated using the following steps:

Step 1: Obtain X, Y, $\hat{A}_c$, $\hat{B}_c$, $\hat{C}_c$ by solving LMIs (12)–(15).

Step 2: Calculate M and N using the relation $MN^T = I - XY$.

Step 3: Obtain the feedback control and triggering parameters η_y, η_u as follows:

$$\begin{aligned}
\begin{bmatrix} A_c & B_c \\ C_c & 0 \end{bmatrix} &= \begin{bmatrix} N & YB_p \\ 0 & I \end{bmatrix}^{-1} \\
&\quad \times \begin{bmatrix} \hat{A}_c - YA_pX & \hat{B}_c \\ \hat{C}_c & 0 \end{bmatrix} \\
&\quad \times \begin{bmatrix} M^T & 0 \\ C_pX & I \end{bmatrix}^{-1}, \\
\eta_u &= (\mu_u \sigma_u)^{-\frac{1}{2}}, \quad \eta_y = (\mu_y \sigma_y)^{-\frac{1}{2}}.
\end{aligned}$$

Proof: See the Appendix.

Remark 4: In [26], the stability analysis results for a class of nonlinear systems were presented, but the controller design technique using the results was not obtained. [27] designed the controller based on the results of [26] and [28] proposed an improved controller design scheme. However, the controller design techniques were all studies for linear systems. In other words, they are the methods that cannot be applied in the systems with nonlinearity and uncertainty. Theorem 2 in this paper even enables the co-design of the feedback controller and triggering parameters for the uncertain nonlinear systems.

Based on Theorem 2, we derive the following corollary.

Corollary 1: Consider the hybrid system (5) with (6) and its controlled output (7). Suppose that for given real scalars $\alpha_1,\ \alpha_2,\ \alpha_3,\ \gamma_{\bar{d}},\ \lambda_y,\ \lambda_u > 0$, there exist scalars $\beta,\ \mu_y,\ \mu_u,\ \sigma_y,\ \sigma_u,\ \gamma_{\bar{w}} > 0$, and $\rho \geq 0$, matrices $\hat{A}_c,\ \hat{B}_c,\ \hat{C}_c$, and positive definite matrices $X,\ Y,\ H_1,\ H_2,\ H_3$ with appropriate dimensions such that

$$\Psi < 0, \tag{16}$$

and (13)–(15) where $\Psi = \{\Psi_{i,j}\},\ i,j \in \{1,2,\ldots,12\}$ is symmetric and the components of Ψ are the same as those of Ω in Theorem 2.

Then, system (5) with (6) is $\mathcal{L}_2$-stable from $(\bar{w},\bar{d})$ to z with an $\mathcal{L}_2$-gain less than or equal to $\gamma = \sqrt{\max\{\gamma_{\bar{w}},\gamma_{\bar{d}}\}}$. Furthermore, the procedure to obtain the output feedback control law is the same as that described in Theorem 2.

Proof: The proof follows the same procedure as the proof of Theorem 2 with $\Delta A_p = 0$. Thus, this is omitted here.

C. REDUCTION OF THE NUMBER OF TRANSMISSIONS

In this subsection, we present an optimization problem that enables the number of transmissions of y and u to be reduced using the optimized controller. The input and output signals are transmitted if $|e_y|$ and $|e_u|$ violate the thresholds $\eta_y|y|$ and $\eta_u|u|$, respectively, according to the triggering conditions (6). Thus, maximizing η_y and η_u in (6) in the controller design reduces the number of transmissions. Furthermore, maximizing η_y and η_u implies minimizing σ_y, and σ_u, μ_y, and μ_u, in (12)–(15) in Theorem 2. Therefore, for the given positive values $\alpha_1,\ \alpha_2,\ \alpha_3,\ \tilde{\gamma}_{\bar{d}}$, and scalars $\lambda_y,\ \lambda_u$, we can formulate the optimization problem as follows:

$$\begin{aligned} &\text{minimize}\ \ \delta_1\mu_y + \delta_2\mu_u + \delta_3\sigma_y + \delta_4\sigma_u \\ &\text{subject to}\ \ (12)\text{–}(15) \end{aligned} \tag{17}$$

where $\delta_1,\ \delta_2,\ \delta_3$, and $\delta_4 \geq 0$ are weight values. The values can be determined by considering the limitations such as hardware characteristics of each channel, communication periods of controllers and actuators, and performance of the ETMs, which may commonly occur in real-world applications. In fact, when there is a limit to triggering of the actuator due to the hardware limitation, relatively large values of η_u and T_u can be obtained by determining large values of δ_2 and δ_4, which can reduce the number of triggering of the actuator.

TABLE 1. η_y, η_u and $\bar{T}_y$, $\bar{T}_u$ obtained using Theorem 1 over various θ.

θ	η_y	T_y	η_u	T_u
0.1	0.2253	0.0735	0.2339	0.0718
0.3	0.1209	0.0510	0.1255	0.0544
0.5	0.0298	0.0309	0.0241	0.0280

TABLE 2. Scalar parameters used for the example in Section 4.1 over various θ.

θ	α_1	α_2	α_3	ρ	ν
0.1	4×10^{-4}	0.6319	3.4986	0.8637	10.4176
0.3	5×10^{-4}	0.6510	4.5911	0.8197	3.5768
0.5	7×10^{-4}	0.6748	5.7745	0.7634	2.2470

For systems without model uncertainties, we can alternatively use (16) in Corollary 1 instead of (12). In Section IV-B, (16) is used for the optimization problem (17) for comparison with previous studies.

IV. NUMERICAL EXAMPLES

A. ROBUST STABILIZATION OF SYSTEMS WITH UNCERTAINTY

We consider the following nonlinear uncertain plant model, modified from the example in [40]:

$$\begin{aligned} \dot{x}_{p1} &= x_{p2}, \\ \dot{x}_{p2} &= -2x_{p1} - 3x_{p2} + \theta\sin(5t)x_{p1} \\ &\quad - \sin(3x_{p1}) + u + w, \\ y &= x_{p1}. \end{aligned}$$

Here, θ is a known constant and used for discussions. According to (5) and (7), we can rewrite the plant model and controlled output as follows:

$$\begin{aligned} &A_{p0} = \begin{bmatrix} 0 & 1 \\ -2 & -3 \end{bmatrix}, \quad E_{p\Delta} = \begin{bmatrix} 0 \\ \theta \end{bmatrix}, \quad F_{p\Delta} = \begin{bmatrix} 1 & 0 \end{bmatrix}, \\ &\Delta_p = \sin(5t), \quad B_f = \begin{bmatrix} 0 \\ -1 \end{bmatrix}, \quad f(x_p) = \sin(3x_{p1}), \\ &B_p = \begin{bmatrix} 0 \\ 1 \end{bmatrix}, \quad E_p = \begin{bmatrix} 0 \\ 1 \end{bmatrix}, \quad C_p = \begin{bmatrix} 1 & 0 \end{bmatrix}, \\ &C_z^p = \begin{bmatrix} 1 & 0.5 \end{bmatrix}, \quad D_z = \begin{bmatrix} 0.5 & 0 & 0 \end{bmatrix}. \end{aligned}$$

We set $\lambda_u = \lambda_y = 0.1$, and $\delta_i = 1,\ i = \{1,2,3,4\}$. To select the parameters α_i for $i \in \{1,2,3\}$, ρ and ν, we can use several optimization methods. In this study, we used `fminsearch` of MATLAB (see [41], [42]). Given $\theta = 0.1$ and $\gamma = 1.5$, the obtained values were $\alpha_1 = 0.0004$, $\alpha_2 = 0.6319$, $\alpha_3 = 3.4986$, $\rho = 0.8637$, and $\nu = 10.4176$.

Here, we set $\gamma_{\bar{w}} = \gamma_{\bar{d}} = \gamma^2$. Then, we can obtain the following control and triggering laws as follows by solving (17):

$$\begin{aligned} &A_c = \begin{bmatrix} -1.7214 & -1.6453 \\ 4.1954 & -4.4467 \end{bmatrix}, \quad B_c = \begin{bmatrix} -0.1656 \\ 4.2723 \end{bmatrix} \\ &C_c = \begin{bmatrix} 0.1754 & -1.4923 \end{bmatrix}, \\ &\eta_y = 0.2253, \quad \eta_u = 0.2339. \end{aligned}$$

TABLE 3. The average number of events on the output channel N^y_{avg} and input channel N^u_{avg}; the average inter-event time on the output channel τ^y_{avg} and input channel τ^u_{avg} for various θ.

θ	N^y_{avg}	τ^y_{avg}	N^u_{avg}	τ^u_{avg}
0.1	43.4	0.1166	56.2	0.0886
0.3	72.6	0.0694	80.34	0.0619
0.5	183.0	0.0273	167.4	0.0298

TABLE 4. Comparison of η_y and η_u between the previous and proposed studies.

	η_y	η_u
Abdelrahim et al. [26]	0.0036	0.0232
Corollary 1	0.0199	0.1358

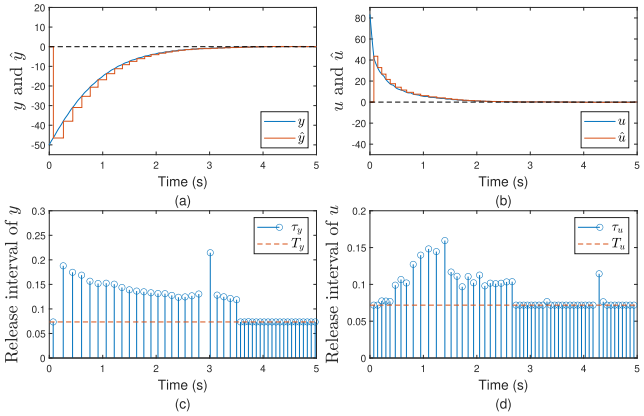

FIGURE 3. (a) The trajectories of $y(t)$ and $\hat{y}(t)$, (b) The trajectories of $u(t)$ and $\hat{u}(t)$; the release intervals of (c) y and (d) u of Theorem 2.

Table 1 shows η_y, $\bar{T}_y$, η_u, and $\bar{T}_y$ values over various values of θ; the scalar parameters used for solving the optimization (17) are presented in Table 2. We observed that η_y, $\bar{T}_y$, η_u, and $\bar{T}_u$ decreased as θ decreased, implying that smaller thresholds in triggering conditions need to be used for the larger influence of the time-varying uncertainties.

We set the initial values $x(0,0) = (-50, 50, 50, -50)$, $e(0,0) = (0,0)$, and $\tau(0,0) = (0,0)$ for the time-domain simulation. The unknown exogenous disturbance w of the plant satisfies $|w(t)| \leq 0.5$, and the noise on the output and control input is $d_y(t) = 0.08\sin(50t)$ and $d_u(t) = 0.1\sin(60t)$, respectively for any $t \geq 0$. Fig. 3 shows the time-domain simulation results for $\theta = 0.1$. The designed ETC effectively stabilized the closed-loop system, reducing the number of transmissions on both channels. Table 3 shows the number of transmissions, and average inter-event times of y and u over various θ with randomly generated initial conditions, $\|x(0,0)\|_2 \leq 100$. This shows that the number of transmissions on both channels increases as the influence of the time-varying uncertainties increases. The largest θ ensuring the LMIs feasible was 5.703.

B. COMPARISON WITH THE PREVIOUS RESULT

Consider the following dynamics of a single-link robot arm, illustrated in [26].

$$\dot{x}_{p1} = x_{p2}, \quad \dot{x}_{p2} = -\sin(x_{p1}) + u + w,$$
$$y = x_{p1}$$

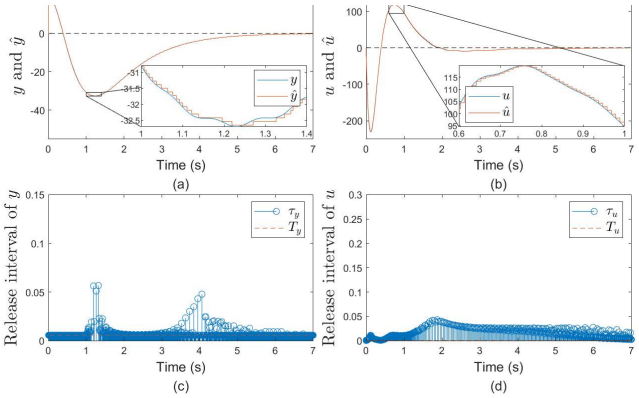

FIGURE 4. (a) The trajectories of $y(t)$ and $\hat{y}(t)$, (b) The trajectories of $u(t)$ and $\hat{u}(t)$; the release intervals of (c) y and (d) u of [26].

Following the representation of (5) and (7), the single-link robot arm can be represented as:

$$A_p = \begin{bmatrix} 0 & 1 \\ 0 & 0 \end{bmatrix}, \quad B_f = \begin{bmatrix} 0 \\ -1 \end{bmatrix} \quad f(x_p) = \sin(x_{p1}),$$
$$B_p = \begin{bmatrix} 0 \\ 1 \end{bmatrix}, \quad E_p = \begin{bmatrix} 0 \\ 1 \end{bmatrix}, \quad C_p = \begin{bmatrix} 1 & 0 \end{bmatrix},$$
$$C_z^p = \begin{bmatrix} 1 & 0.5 \end{bmatrix}, \quad D_z = \begin{bmatrix} 0.5 & 0 & 0 \end{bmatrix}.$$

We chose $\lambda_u = 0.01$, $\lambda_y = 1$, and $\gamma = 19.3746$, which were used in [26]. We set $\gamma_{\bar{w}} = \gamma_{\bar{d}} = \gamma^2$. We chose $\delta_1 = \delta_3 = 1$, $\delta_2 = \delta_4 = 50$. Using the same method as in the previous subsection, we obtained $\alpha_1 = 0.0883, \alpha_2 = 0.0835$, $\alpha_3 = 44.9565$, and $\rho = 4.8263$. Table 4 shows that the η_y and η_u obtained using the proposed conditions are larger than those of the previous study. The larger values can increase the time required for the event-triggering rule to be violated, that is, it can increase the inter-transmission times.

The obtained upper bounds of T_y and T_u are 6.79×10^{-2} and 5.59×10^{-3}, respectively. Note that the upper bounds of T_y and T_u obtained by the previously published method were 5.62×10^{-3} and 3.63×10^{-4}, respectively, which are smaller than those of the proposed method. The parameters of the controller are obtained as follows:

$$A_c = \begin{bmatrix} -5.2307 & -14.6627 \\ 4.2807 & -18.2182 \end{bmatrix}, \quad B_c = \begin{bmatrix} -29.5269 \\ 152.5669 \end{bmatrix}$$
$$C_c = \begin{bmatrix} -0.4920 & -2.3653 \end{bmatrix}.$$

For the time-domain simulation, the unknown exogenous disturbance w is applied, satisfying $|w(t)| \leq 0.1$; the noise signals on the output and control input are $d_y(t) = 0.08\sin(60t)$ and $d_u(t) = 0.1\sin(50t)$, respectively. We set $T_y = 1.70 \times 10^{-2}$ and $T_u = 5.59 \times 10^{-3}$. Figs. 4 and 5 shows the time-domain simulation results of the previous and proposed methods for the initial values $x(0,0) = (20, -20, -20, 20)$, $e(0,0) = (0,0)$, and $\tau(0,0) = (0,0)$. We observe that the number of data transmissions of the proposed method was significantly less than those of [26]. Furthermore, we also see that the controller obtained using

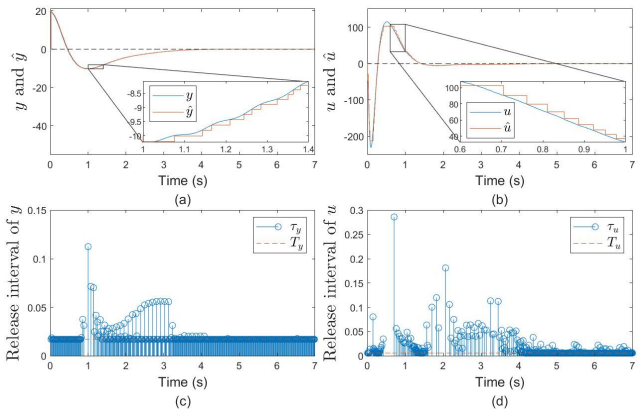

FIGURE 5. (a) The trajectories of $y(t)$ and $\hat{y}(t)$, (b) The trajectories of $u(t)$ and $\hat{u}(t)$; the release intervals of (c) y and (d) u of Corollary 1.

TABLE 5. The average number of events on the output (N^y_{avg}) and input (N^u_{avg}) channels; the average inter-event time on the output (τ^y_{avg}) and input (τ^u_{avg}) channels per simulation.

	N^y_{avg}	τ^y_{avg}	N^u_{avg}	τ^u_{avg}
Abdelrahim et al. [26]	1637.0	0.0061	4401.9	0.0027
Corollary 1	542.5	0.0184	1006.25	0.0101

the proposed method shows better transient performance in the output y.

Table 5 summarizes the number of transmissions of y and u, and the average inter-event times of y and u for 10 s with randomly generated initial conditions such that $\|x(0,0)\|_2 \leq 100$. The number of transmissions of y and u in the proposed method is 33.14% and 22.86% of those of the previously published method in the simulation, respectively. The inter-event times of the output and input of the proposed method are 301.64% and 374.07% of those of the previously published method at the same guaranteed $\mathcal{L}_2$-gain.

V. CONCLUSION

This paper has proposed a co-design of the DOF and event-triggering laws for nonlinear uncertain systems. ETC systems including the nonlinear uncertain plant output and dynamic output controller transmitting the measurement and control signals using their sampling rules have been described as hybrid dynamical systems. As the nonlinear plant is affected by time-varying uncertainties, the error dynamics of the recently transmitted and currently measured signals have also included these uncertainties making the controller design difficult. First, we have presented $\mathcal{L}_2$-stability analysis of ETC systems. Subsequently, based on the analysis, we have proposed LMI-based design conditions for the DOF and event-triggering laws. We have deduced LMI-based conditions using the modified Young's inequality and the elimination of uncertainties. The proposed design method can minimize the number of transmissions by solving a convex optimization problem. The simulation results have shown that proposed method effectively design the controller to stabilize the uncertain nonlinear network system. Furthermore, the controller designed by the proposed method has greatly reduced the number of transmissions of the ETC system, compared to the previous study. In future research, the authors will be devoted to the robust output feedback event-triggering control schemes for a class of the uncertain systems with nonlinearity that does not guarantee the global Lipschitz condition. Furthermore, the co-design of static output feedback controller and event-triggering condition for a class of uncertain nonlinear systems is still an open problem and would be an interesting research direction.

APPENDIX

Before we present proofs, we introduce the following lemmas that are necessary for the proof of Theorem 1 and 2.

Lemma 2 [43]: Let $V_0(\zeta)$ and $V_1(\zeta)$ be two arbitrary quadratic forms over $\mathbb{R}^n$. Then $V_0(\zeta) < 0$ is a consequence of $V_1(\zeta) \leq 0$ if and only if there exists $\rho \geq 0$ such that

$$V_0(\zeta) < \rho V_1(\zeta), \quad \forall\, \zeta \in \mathbb{R}^n - \{0\}.$$

Lemma 3 [44]: Given constant matrices $\mathcal{M}, \mathcal{N}, \mathcal{Y}$; positive semi-definite matrix R with appropriate dimensions and $\mathcal{Y} = \mathcal{Y}^T$, then for any Δ satisfying $\Delta^T\Delta \leq \mathcal{R}$, the following inequality holds:

$$\mathcal{Y} + \mathcal{M}\Delta\mathcal{N} + \mathcal{N}^T\Delta^T\mathcal{M}^T < 0$$

if and only if there exists a constant $\nu > 0$ such that:

$$\mathcal{Y} + \nu\mathcal{M}\mathcal{M}^T + \nu^{-1}\mathcal{N}^T\mathcal{R}\mathcal{N} < 0.$$

Lemma 4 [28]: For given matrix $\mathcal{X} \in \mathbb{R}^{n\times n}$, the following inequality is satisfied for any matrix $S > 0$ and scalar α,

$$\alpha\left(\mathcal{X}^T + \mathcal{X}\right) - \mathcal{X}^T S\mathcal{X} \leq \alpha^2 S^{-1}.$$

Proof of Theorem 1: Let $W_y(e_y) = \lambda_y|e_y|$ and $W_u(e_u) = \lambda_u|e_u|$. Then, for almost all $e \in \mathbb{R}^{n_e}$ and all $(x,\xi) \in \mathbb{R}^{n_x+n_\xi}$, we have

$$\begin{aligned}\langle\nabla W_y(e_y), \bar{f}_2(x,e,\xi)\rangle &\leq \lambda_y|A_2x + R_2f(x_p) \\ &\quad + M_2e_u + E_2\bar{w} + F_2\bar{d}|, \\ \langle\nabla W_u(e_u), \bar{f}_3(x,e,\xi)\rangle &\leq \lambda_y|A_3x + M_3e_y + E_3\bar{w} + F_3\bar{d}|.\end{aligned}$$

Hence, condition (10) holds with $L_y = 0$, $H_y(x,e_u,\xi) = \lambda_y|A_2x+R_2f(x_p)+M_2e_u+E_2\bar{w}+F_2\bar{d}|, L_u = 0, H_u(x,e_y,\xi) = \lambda_u|A_3x + M_3e_y + E_3\bar{w} + F_3\bar{d}|$, and $L_u = 0$.

Let $V(x) = x^TPx$, for $x \in \mathbb{R}^{n_x}$. (8) is satisfied with $\underline{\alpha}(s) = \lambda_{min}(P)s^2$ and $\overline{\alpha}(s) = \lambda_{max}(P)s^2$ for $s \geq 0$. And it holds that $\langle\nabla V(x), \bar{f}_1(x,e,\xi)\rangle = x^T(A_1^TP + PA_1)x + (R_1f(x_p) + B_1e_y + M_1e_u + E_1\bar{w})^TPx + x^TP(R_1f(x_p) + B_1e_y + M_1e_u + E_1\bar{w})$ for almost all $x \in \mathbb{R}^{n_x}$ and all $(e,\xi) \in \mathbb{R}^{n_e+n_\xi}$. Let us define the state vector $\zeta := (x, f(x_p), e_y, e_u, \bar{w}, \bar{d})$. Because $f(x_p)$ is β-Lipschitz, we have

$$f(x_p)^Tf(x_p) \leq \beta x_p^Tx_p \Leftrightarrow \zeta^T\Upsilon\zeta \leq 0, \tag{18}$$

where $\Upsilon := \text{diag}\{-\beta U_p^TU_p, I, 0, 0, 0, 0\}$. Post-and pre-multiplying (11) by ζ and its transpose, we have $\zeta^T\Psi\zeta$.

Applying Lemma 2 with $V_0(\zeta) = \zeta^T \Psi \zeta$ and $V_1(\zeta) = \zeta^T \Upsilon \zeta$ in (18) yields

$$\begin{aligned}\langle \nabla V(x), \bar{f}_1(x,e,\xi)\rangle \leq & -|z|^2 + \eta_{\bar{w}}^2|\bar{w}|^2 + \eta_{\bar{d}}^2|\bar{d}|^2 - \varepsilon_y|y|^2 \\ & - \varepsilon_u|u|^2 + \gamma_y^2 W_y^2(e_y) + \gamma_u^2 W_u^2(e_u) \\ & - H_y^2(x,e_u,\xi) - H_u^2(x,e_y,\xi)\end{aligned}$$

where $\eta_{\bar{w}}^2 = \gamma_{\bar{d}}$, $\eta_{\bar{d}}^2 = \gamma_{\bar{d}}$, $\gamma_y^2 = \frac{\mu_y}{\lambda_y^2}$, and $\gamma_u^2 = \frac{\mu_u}{\lambda_u^2}$. Thus, (9) is verified with $\delta_y(y) = \varepsilon_y|y|^2$, $\delta_u(u) = \varepsilon_u|u|^2$. □

Proof of Theorem 2: Let us define the positive definite matrix $P \in \mathbb{R}^{n_x+n_c}$,

$$T_1 = \begin{bmatrix} Y & I \\ N^T & 0 \end{bmatrix}, \quad T_2 = \begin{bmatrix} I & X \\ 0 & M^T \end{bmatrix}$$

such that $T_1 = PT_2$ and $MN^T = I - XY$. Then, we can obtain $T_1^T A_{10} T_2 = \Phi_1$, $R_1^T T_1 = \Phi_2$, $B_1^T T_1 = \Phi_3$, $M_1^T T_1 = \Phi_4$, $E_1^T T_1 = \Phi_5$, $C_y T_2 = \Phi_6$, $C_u T_2 = \Phi_7$, $C_z T_2 = \Phi_8$, $U_p T_2 = \Phi_9$, $E_\Delta^T T_1 = \Phi_{10}$, $F_\Delta T_2 = \Phi_{11}$, $T_1^T T_2 = \Phi_{12}$ where

$$\left[\begin{array}{cccccccccccc|cc}
PA_{10}+A_{10}^TP & \star & \star & \star & \star & \star & \star & \star & \star & \star & \star & \star & \star & \star \\
R_1^TP & -\rho I & \star & \star & \star & \star & \star & \star & \star & \star & \star & \star & \star & \star \\
B_1^TP & 0 & -\mu_y I & \star & \star & \star & \star & \star & \star & \star & \star & \star & \star & \star \\
M_1^TP & 0 & 0 & -\mu_u I & \star & \star & \star & \star & \star & \star & \star & \star & \star & \star \\
E_1^TP & 0 & 0 & 0 & -\gamma_{\bar{w}} I & \star & \star & \star & \star & \star & \star & \star & \star & \star \\
PA_{10} & PR_1 & PB_1 & PM_1 & PE_1 & \mathcal{S}_1 & \star & \star & \star & \star & \star & \star & \star & \star \\
PA_{10} & PR_1 & 0 & PM_1 & PE_1 & 0 & \mathcal{S}_2 & \star & \star & \star & \star & \star & \star & \star \\
PA_{10} & 0 & PB_1 & 0 & PE_1 & 0 & 0 & \mathcal{S}_3 & \star & \star & \star & \star & \star & \star \\
C_y & 0 & 0 & 0 & D_y & 0 & 0 & 0 & -\sigma_y I & \star & \star & \star & \star & \star \\
C_u & 0 & 0 & 0 & D_u & 0 & 0 & 0 & 0 & -\sigma_u I & \star & \star & \star & \star \\
C_z & 0 & 0 & 0 & D_z & 0 & 0 & 0 & 0 & 0 & -I & \star & \star & \star \\
U_p & 0 & 0 & 0 & 0 & 0 & 0 & 0 & 0 & 0 & 0 & \frac{-1}{\rho\beta} I & \star & \star \\
\hline
E_\Delta^TP & 0 & 0 & 0 & 0 & E_\Delta^TP & E_\Delta^TP & E_\Delta^TP & 0 & 0 & 0 & 0 & \frac{-1}{\nu} I & \star \\
F_\Delta & 0 & 0 & 0 & 0 & 0 & 0 & 0 & 0 & 0 & 0 & 0 & 0 & -\nu I
\end{array}\right] < 0, \tag{19}$$

$$\mathcal{S}_1 = -\frac{\tilde{\gamma}_{\bar{d}}}{\alpha_1^2}\bar{H}_1, \quad \mathcal{S}_2 = -\frac{1}{(\lambda_y\alpha_2)^2}\bar{H}_2, \quad \mathcal{S}_3 = -\frac{1}{(\lambda_u\alpha_3)^2}\bar{H}_3$$

$$\mathcal{Y} + \nu\mathcal{M}\mathcal{M}^T + \nu^{-1}\mathcal{N}^T\mathcal{N} < 0,$$

$$\mathcal{Y} = \left[\begin{array}{ccccccccccc}
PA_{10}+A_{10}^TP & \star & \star & \star & \star & \star & \star & \star & \star & \star & \star \\
R_1^TP & -\rho I & \star & \star & \star & \star & \star & \star & \star & \star & \star \\
B_1^TP & 0 & -\mu_y I & \star & \star & \star & \star & \star & \star & \star & \star \\
M_1^TP & 0 & 0 & -\mu_u I & \star & \star & \star & \star & \star & \star & \star \\
E_1^TP & 0 & 0 & 0 & -\gamma_{\bar{w}} I & \star & \star & \star & \star & \star & \star \\
PA_{10} & PR_1 & PB_1 & PM_1 & PE_1 & \mathcal{S}_1 & \star & \star & \star & \star & \star \\
PA_{10} & PR_1 & 0 & PM_1 & PE_1 & 0 & \mathcal{S}_2 & \star & \star & \star & \star \\
PA_{10} & 0 & PB_1 & 0 & PE_1 & 0 & 0 & \mathcal{S}_3 & \star & \star & \star \\
C_y & 0 & 0 & 0 & D_y & 0 & 0 & 0 & -\sigma_y I & \star & \star \\
C_u & 0 & 0 & 0 & D_u & 0 & 0 & 0 & 0 & -\sigma_u I & \star \\
C_z & 0 & 0 & 0 & D_z & 0 & 0 & 0 & 0 & 0 & -I \\
U_p & 0 & 0 & 0 & 0 & 0 & 0 & 0 & 0 & 0 & \frac{-1}{\rho\beta} I
\end{array}\right],$$

$$\mathcal{M} = \begin{bmatrix} E_\Delta^TP & 0 & 0 & 0 & 0 & E_\Delta^TP & E_\Delta^TP & E_\Delta^TP & 0 & 0 & 0 & 0 \end{bmatrix},$$

$$\mathcal{N} = \begin{bmatrix} F_\Delta & 0 & 0 & 0 & 0 & 0 & 0 & 0 & 0 & 0 & 0 & 0 \end{bmatrix}^T \tag{20}$$

$\hat{A}_c = YA_{p0}X + NB_cC_pX + YB_pC_cM^T + NA_cM^T$, $\hat{B}_c = NB_c$, and $\hat{C}_c = C_cM^T$. Thus, pre- and post-multiplying (12) by a matrix $\mathrm{diag}\{T_2^{-1}, I, I, I, I, T_2^{-1}, T_2^{-1}, T_2^{-1}, I, I, I, I, I, I\}$ and its transpose yields (19), as shown at the bottom of the previous page, where $\bar{H}_1 = T_2^{-T}H_1T_2^{-1}$, $\bar{H}_2 = T_2^{-T}H_2T_2^{-1}$, and $\bar{H}_3 = T_2^{-T}H_3T_2^{-1}$. Applying the Schur complement on (19) yields (20), as shown at the bottom of the previous page. Based on Lemma 3, (21) holds from (20). By applying the Schur complement on (21), as shown at the bottom of the page, we obtain (22), as shown at the bottom of the page, where $\varepsilon_u = \sigma_u^{-1}$ and $\varepsilon_y = \sigma_y^{-1}$. On the other hand, (13) can be rewritten as:

$$\begin{bmatrix} I & \star & \star \\ 0 & I & \star \\ \lambda_y^2 T_2^T C_y^T & \lambda_u^2 T_2^T C_u^T & 2\alpha_1 T_2^T T_1 - H_1 \end{bmatrix} \geq 0. \quad (23)$$

Multiplying the left of (23) by $\mathrm{diag}\{I, I, T_2^{-T}\}$ and the right by its transpose yields

$$\left[\begin{array}{c|c} I & \star \\ \hline G^T & 2\alpha_1 P - \bar{H}_1 \end{array}\right] \geq 0, \quad (24)$$

where $G = \begin{bmatrix} \lambda_y^2 C_p & 0 \\ 0 & \lambda_u^2 C_c \end{bmatrix}$. By applying Schur complement on (24), we have

$$2\alpha_1 P - \bar{H}_1 - G^T G \geq 0.$$

Similarly, one can obtain the following inequalities from the LMIs in (13)–(15):

$$G^T G \leq 2\alpha_1 P - \bar{H}_1, \quad C_y^T C_y \leq 2\alpha_2 P - \bar{H}_2, \quad C_u^T C_u \leq 2\alpha_3 P - \bar{H}_3. \quad (25)$$

$$\left[\begin{array}{ccccc|ccc|cccc} PA_1 + A_1^T P & \star & \star & \star & \star & \star & \star & \star & \star & \star & \star & \star \\ R_1^T P & -\rho I & \star & \star & \star & \star & \star & \star & \star & \star & \star & \star \\ B_1^T P & 0 & -\mu_y I & \star & \star & \star & \star & \star & \star & \star & \star & \star \\ M_1^T P & 0 & 0 & -\mu_u I & \star & \star & \star & \star & \star & \star & \star & \star \\ E_1^T P & 0 & 0 & 0 & -\gamma_{\bar{w}} I & \star & \star & \star & \star & \star & \star & \star \\ \hline PA_1 & PR_1 & PB_1 & PM_1 & PE_1 & \mathcal{S}_1 & \star & \star & \star & \star & \star & \star \\ PA_1 & PR_1 & 0 & PM_1 & PE_1 & 0 & \mathcal{S}_2 & \star & \star & \star & \star & \star \\ PA_1 & 0 & PB_1 & 0 & PE_1 & 0 & 0 & \mathcal{S}_3 & \star & \star & \star & \star \\ \hline C_y & 0 & 0 & 0 & D_y & 0 & 0 & 0 & -\sigma_y I & \star & \star & \star \\ C_u & 0 & 0 & 0 & D_u & 0 & 0 & 0 & 0 & -\sigma_u I & \star & \star \\ C_z & 0 & 0 & 0 & D_z & 0 & 0 & 0 & 0 & 0 & -I & \star \\ U_p & 0 & 0 & 0 & D_z & 0 & 0 & 0 & 0 & 0 & 0 & -(\rho\beta)^{-1} I \end{array}\right] < 0 \quad (21)$$

$$\begin{bmatrix} \Xi_1 & \star & \star & \star & \star \\ R_1^T P & -\rho I & \star & \star & \star \\ B_1^T P & 0 & -\mu_y I & \star & \star \\ M_1^T P & 0 & 0 & -\mu_u I & \star \\ \Xi_2 & 0 & 0 & 0 & \Xi_3 \end{bmatrix} + \begin{bmatrix} A_1^T P & A_1^T P & A_1^T P \\ R_1^T P & R_1^T P & 0 \\ B_1^T P & 0 & B_1^T P \\ M_1^T P & M_1^T P & 0 \\ E_1^T P & E_1^T P & E_1^T P \end{bmatrix} \Xi_4 \begin{bmatrix} PA_1 & PR_1 & PB_1 & PM_1 & PE_1 \\ PA_1 & PR_1 & 0 & PM_1 & PE_1 \\ PA_1 & 0 & PB_1 & 0 & PE_1 \end{bmatrix} < 0,$$

$$\Xi_1 = PA_1 + A_1^T P + C_z^T C_z + \varepsilon_y C_y^T C_y + \varepsilon_u C_u^T C_u + \rho\beta U_p^T U_p, \ \Xi_2 = E_1^T P + D_z^T C_z + \varepsilon_y D_y^T C_y + \varepsilon_u D_u^T C_u,$$
$$\Xi_3 = -\gamma_{\bar{w}} I + D_z^T D_z + \varepsilon_y D_y^T D_y + \varepsilon_u D_u^T D_u, \ \Xi_4 = \mathrm{diag}(\tilde{\gamma}_{\bar{d}}^{-1}\alpha_1^2 \bar{H}_1^{-1}, \ (\lambda_y\alpha_2)^2 \bar{H}_2^{-1}, \ (\lambda_u\alpha_3)^2 \bar{H}_3^{-1}) \quad (22)$$

$$\begin{bmatrix} \Xi_1 & \star & \star & \star & \star \\ R_1^T P & -\rho I & \star & \star & \star \\ B_1^T P & 0 & -\mu_y I & \star & \star \\ M_1^T P & 0 & 0 & -\mu_u I & \star \\ \Xi_2 & 0 & 0 & 0 & \Xi_3 \end{bmatrix} + \begin{bmatrix} A_1^T & A_1^T & A_1^T \\ R_1^T & R_1^T & 0 \\ B_1^T & 0 & B_1^T \\ M_1^T & M_1^T & 0 \\ E_1^T & E_1^T & E_1^T \end{bmatrix} \Xi_5 \begin{bmatrix} A_1 & R_1 & B_1 & M_1 & E_1 \\ A_1 & R_1 & 0 & M_1 & E_1 \\ A_1 & 0 & B_1 & 0 & E_1 \end{bmatrix} < 0,$$
$$\Xi_5 = \mathrm{diag}(\tilde{\gamma}_{\bar{d}}^{-1} G^T G, \ \lambda_y^2 C_y^T C_y, \ \lambda_u^2 C_u^T C_u) \quad (27)$$

Pre- and post-multiplying the inequalities in (25) by P^{-1} yields by Lemma 4:

$$\begin{aligned} P^{-1}G^T GP^{-1} &\leq 2\alpha_1 P^{-1} - P^{-1}\bar{H}_1 P^{-1} \leq \alpha_1^2 \bar{H}_1^{-1}, \\ P^{-1}C_y^T C_y P^{-1} &\leq 2\alpha_2 P - P^{-1}\bar{H}_2 P^{-1} \leq \alpha_2^2 \bar{H}_2^{-1}, \\ P^{-1}C_u^T C_u P^{-1} &\leq 2\alpha_3 P^{-1} - P^{-1}\bar{H}_3 P^{-1} \leq \alpha_3^2 \bar{H}_3^{-1}. \end{aligned} \quad (26)$$

Thus, (27), as shown at the bottom of the previous page, is satisfied from (22) and (26). Applying the Schur complement on (27), we have (11) in Theorem 1 with $GA_1 = \lambda_y^2 F_2^T A_2 + \lambda_u^2 F_3^T A_3$, $GR_1 = \lambda_y^2 F_2^T R_2$, $GB_1 = \lambda_u^2 F_3^T B_3$, $GM_1 = \lambda_y^2 F_2^T M_2$, $GE_1 = \lambda_y^2 F_2^T E_2 + \lambda_u^2 F_3^T E_3$ and $\tilde{\gamma}_{\bar{d}} I = \gamma_{\bar{d}} I - \lambda_y^2 F_2^T F_2 - \lambda_u^2 F_3^T F_3$. Thus, we can conclude that the system (5) with (6) is $\mathcal{L}_2$ stable from $(\bar{w}, \bar{d})$ to z with an $\mathcal{L}_2$ gain less than or equal to $\gamma = \sqrt{\max\{\gamma_{\bar{w}}, \gamma_{\bar{d}}\}}$. □

REFERENCES

[1] J. Nilsson, "Real-time control systems with delays," Ph.D. dissertation, Dept. Autom. Control, Lund Inst. Technol. (LTH), Lund, Sweden, 1998.

[2] W. Zhang, M. S. Branicky, and S. M. Phillips, "Stability of networked control systems," *IEEE Control Syst. Mag.*, vol. 21, no. 1, pp. 84–99, Feb. 2001.

[3] G. C. Walsh, H. Ye, and L. G. Bushnell, "Stability analysis of networked control systems," *IEEE Trans. Control Syst. Technol.*, vol. 10, no. 3, pp. 438–446, May 2002.

[4] Y. Tipsuwan and M.-Y. Chow, "Control methodologies in networked control systems," *Control Eng. Pract.*, vol. 11, no. 10, pp. 1099–1111, Oct. 2003.

[5] D. Hristu-Varsakelis and W. S. Levine, *Handbook of Networked and Embedded Control Systems*. Boston, MA, USA: Birkhäuser, 2005.

[6] Z. Mao and B. Jiang, "Fault identification and fault-tolerant control for a class of networked control systems," *Int. J. Innov. Comput., Inf. Control*, vol. 3, no. 5, pp. 1121–1130, Oct. 2007.

[7] Y. Wang and Z. Sun, "H_∞ control of networked control system via LMI approach," *Int. J. Innov. Comput., Inf. Contr.*, vol. 3, no. 2, pp. 343–352, Apr. 2007.

[8] Y. Shi, H. Fang, and M. Yan, "Kalman filter-based adaptive control for networked systems with unknown parameters and randomly missing outputs," *Int. J. Robust Nonlinear Control*, vol. 19, no. 18, pp. 1976–1992, Dec. 2009.

[9] X.-M. Zhang, Q.-L. Han, and X. Yu, "Survey on recent advances in networked control systems," *IEEE Trans. Ind. Informat.*, vol. 12, no. 5, pp. 1740–1752, Oct. 2016.

[10] M. Mazo and P. Tabuada, "Decentralized event-triggered control over wireless sensor/actuator networks," *IEEE Trans. Autom. Control*, vol. 56, no. 10, pp. 2456–2461, Oct. 2011.

[11] D. V. Dimarogonas, E. Frazzoli, and K. H. Johansson, "Distributed event-triggered control for multi-agent systems," *IEEE Trans. Autom. Control*, vol. 57, no. 5, pp. 1291–1297, May 2012.

[12] W. P. M. H. Heemels, A. R. Teel, N. van de Wouw, and D. Nešić, "Networked control systems with communication constraints: Tradeoffs between transmission intervals, delays and performance," *IEEE Trans. Autom. Control*, vol. 55, no. 8, pp. 1781–1796, Aug. 2010.

[13] J. Liang, K. Liu, Z. Ji, and X. Wang, "Event-triggered consensus control for linear multi-agent systems," *IEEE Access*, vol. 7, pp. 144572–144579, 2019.

[14] J.-Y. Jhang, J.-L. Wu, and C.-F. Yung, "Design of event-triggered state-constrained stabilizing controllers for nonlinear control systems," *IEEE Access*, vol. 10, pp. 3659–3667, 2022.

[15] H. Pan, D. Zhang, W. Sun, and X. Yu, "Event-triggered adaptive asymptotic tracking control of uncertain MIMO nonlinear systems with actuator faults," *IEEE Trans. Cybern.*, early access, Mar. 17, 2021, doi: 10.1109/TCYB.2021.3061888.

[16] J. Wang, H. Pan, and W. Sun, "Event-triggered adaptive fault-tolerant control for unknown nonlinear systems with applications to linear motor," *IEEE/ASME Trans. Mechatronics*, vol. 27, no. 2, pp. 940–949, Apr. 2022.

[17] H. Pan, X. Chang, and D. Zhang, "Event-triggered adaptive control for uncertain constrained nonlinear systems with its application," *IEEE Trans. Ind. Informat.*, vol. 16, no. 6, pp. 3818–3827, Jun. 2020.

[18] Z.-M. Li, X.-H. Chang, and J. H. Park, "Quantized static output feedback fuzzy tracking control for discrete-time nonlinear networked systems with asynchronous event-triggered constraints," *IEEE Trans. Syst., Man, Cybern. Syst.*, vol. 51, no. 6, pp. 3820–3831, Jun. 2021.

[19] M. Donkers and W. Heemels, "Output-based event-triggered control with guaranteed L_∞-gain and improved event-triggering," in *Proc. 49th IEEE Conf. Decis. Cont. (CDC)*, Dec. 2010, pp. 3246–3251.

[20] R. Postoyan, P. Tabuada, D. Nešić, and A. Anta, "A framework for the event-triggered stabilization of nonlinear systems," *IEEE Trans. Autom. Control*, vol. 60, no. 4, pp. 982–996, Apr. 2015.

[21] M. Davoodi, N. Meskin, and K. Khorasani, "Event-triggered multiobjective control and fault diagnosis: A unified framework," *IEEE Trans. Ind. Informat.*, vol. 13, no. 1, pp. 298–311, Feb. 2017.

[22] F. Li, J. Fu, and D. Du, "An improved event-triggered communication mechanism and L_∞ control co-design for network control systems," *Inf. Sci.*, vols. 370–371, pp. 743–762, Nov. 2016.

[23] X. Meng and T. Chen, "Event detection and control co-design of sampled-data systems," *Int. J. Control*, vol. 87, no. 4, pp. 777–786, 2014.

[24] X.-M. Zhang and Q.-L. Han, "Event-based dynamic output feedback control for networked control systems," in *Proc. Amer. Control Conf.*, Jun. 2013, pp. 3008–3013.

[25] X.-H. Chang, C. Yang, and J. Xiong, "Quantized fuzzy output feedback H_∞ control for nonlinear systems with adjustment of dynamic parameters," *IEEE Trans. Syst., Man, Cybern. Syst.*, vol. 49, no. 10, pp. 2005–2015, Sep. 2019.

[26] M. Abdelrahim, R. Postoyan, J. Daafouz, and D. Nešić, "Robust event-triggered output feedback controllers for nonlinear systems," *Automatica*, vol. 75, pp. 96–108, Jan. 2017.

[27] M. Abdelrahim, R. Postoyan, J. Daafouz, D. Nesic, and M. Heemels, "Co-design of output feedback laws and event-triggering conditions for the L_2-stabilization of linear systems," *Automatica*, vol. 87, pp. 337–344, Jan. 2018.

[28] J. Ban, M. Seo, T. Goh, H. Jeong, and S. W. Kim, "Improved co-design of event-triggered dynamic output feedback controllers for linear systems," *Automatica*, vol. 111, Jan. 2020, Art. no. 108600.

[29] W.-H. Chen, D. J. Ballance, P. J. Gawthrop, and J. O'Reilly, "A nonlinear disturbance observer for robotic manipulators," *IEEE Trans. Ind. Electron.*, vol. 47, no. 4, pp. 932–938, Aug. 2000.

[30] S. Li and Z. Liu, "Adaptive speed control for permanent-magnet synchronous motor system with variations of load inertia," *IEEE Trans. Ind. Electron.*, vol. 56, no. 8, pp. 3050–3059, Aug. 2009.

[31] J. Sun, J. Yang, W. X. Zheng, and S. Li, "GPIO-based robust control of nonlinear uncertain systems under time-varying disturbance with application to DC–DC converter," *IEEE Trans. Circuits Syst. II, Exp. Briefs*, vol. 63, no. 11, pp. 1074–1078, Nov. 2016.

[32] S. Jeong and J. Ban, "Robust dynamic output feedback event-triggering synchronization for complex dynamical networks," *IEEE Access*, vol. 10, pp. 51261–51271, 2022.

[33] D. P. Borgers and W. P. M. H. Heemels, "Event-separation properties of event-triggered control systems," *IEEE Trans. Autom. Control*, vol. 59, no. 10, pp. 2644–2656, Oct. 2014.

[34] J. Yang, J. Sun, W. X. Zheng, and S. Li, "Periodic event-triggered robust output feedback control for nonlinear uncertain systems with time-varying disturbance," *Automatica*, vol. 94, pp. 324–333, Aug. 2018.

[35] A. J. Van Der Schaft and J. M. Schumacher, *An Introduction to Hybrid Dynamical Systems*, vol. 251. London, U.K.: Springer 2000.

[36] R. Goebel, R. G. Sanfelice, and A. R. Teel, *Hybrid Dynamical Systems*. Princeton, NJ, USA: Princeton Univ. Press, 2012.

[37] D. Zhang, Q.-L. Han, and X. Jia, "Network-based output tracking control for T–S fuzzy systems using an event-triggered communication scheme," *Fuzzy Sets Syst.*, vol. 273, pp. 26–48, Aug. 2015.

[38] Y. Pan and G.-H. Yang, "Event-based output tracking control for fuzzy networked control systems with network-induced delays," *Appl. Math. Comput.*, vol. 346, pp. 513–530, Apr. 2019.

[39] Z. Gu, D. Yue, J. Liu, and Z. Ding, "H_∞ tracking control of nonlinear networked systems with a novel adaptive event-triggered communication scheme," *J. Franklin Inst.*, vol. 354, no. 8, pp. 3540–3553, 2017.

[40] M. Donkers and W. Heemels, "Output-based event-triggered control with guaranteed L_∞-gain and improved and decentralized event-triggering," *IEEE Trans. Autom. Control*, vol. 57, no. 6, pp. 1362–1376, Jun. 2011.

[41] L. Xie, L. Lu, D. Zhang, and H. Zhang, "Improved robust H_2 and H_∞ filtering for uncertain discrete-time systems," *Automatica*, vol. 40, no. 5, pp. 873–880, May 2004.

[42] J. C. Lagarias, J. A. Reeds, M. H. Wright, and P. E. Wright, "Convergence properties of the Nelder–Mead simplex method in low dimensions," *SIAM J. Optim.*, vol. 9, no. 1, pp. 112–147, 1998.
[43] S. Boyd, L. El Ghaoui, E. Feron, and V. Balakrishnan, *Linear Matrix Inequalities in System and Control Theory*. Philadelphia, PA, USA: SIAM, 1994.
[44] L. Xie, "Output feedback H_∞ control of systems with parameter uncertainty," *Int. J. Contr.*, vol. 63, no. 4, pp. 741–750, 1996.

SEONGCHEOL JEONG was born in Busan, South Korea, in 1981. He received the B.S. degree in electronic and electrical engineering from Busan National University, Busan, in 2008, and the Ph.D. degree in electrical engineering from POSTECH, Pohang, South Korea, in 2013.

His current research interests include control theory, hybrid dynamical systems, complex dynamical systems, event-triggering control, fuzzy disturbance observer, and robust adaptive control.

JAEPIL BAN (Member, IEEE) received the Ph.D. degree in electrical engineering from the Pohang University of Science and Technology, Pohang, South Korea, in 2020.

From 2020 to August 2021, he was a Postdoctoral Researcher with the Pohang University of Science and Technology. Since 2021, he has been an Assistant Professor with the Kumoh National Institute of Technology. His research interests include power system control, application of reinforcement learning, and state and line parameter estimation.

HARIM LEE received the B.S. degree in electrical engineering from Kyungpook National University, Daegu, South Korea, in 2013, the M.S. degree in IT convergence engineering from the Pohang University of Science and Technology (POSTECH), Pohang, South Korea, in 2015, and the Ph.D. degree from the School of Electrical and Computer Engineering, Ulsan National Institute of Science and Technology (UNIST), Ulsan, South Korea, in August 2020. From September 2020 to August 2021, he worked as a Postdoctoral Researcher with the Department of Electrical Engineering, POSTECH. Since September 2021, he has been an Assistant Professor with the School of Electronic Engineering, Kumoh National Institute of Technology, Gumi, South Korea. His research interests include autonomous UAV systems, privacy-protecting deep learning, PHY and MAC for the next generation mobile networks, and embedded systems and robotics such as licensed assisted access in LTE (LTE-LAA), wireless networking with deep neural networks, and radar systems. He received the Kwanjeong Educational Foundation Fellowship, from 2013 to 2014.